BIODIVERSITAS
Volume 27, Number 4, April 2026
Pages: 12

ISSN: 1412-033X
E-ISSN: 2085-4722
https://doi.org/10.13057/biodiv/d270439

Landmark-based geometric morphometrics as a complementary tool for female identification of *Euplatypus compositus* and *Euplatypus parallelus*

KIATGAWIN CHATPIYAPHAT[1,2,♥], AKHMAD RIZALI[2], BAMBANG TRI RAHARDJO[2], JIANGUO WANG[3], XU YE[3], WISUT SITTICHAYA[4], ANDREW J. JOHNSON[5], JIRI HULCR[5], HAGUS TARNO[2,♥♥]

[1]Doctoral Program in Agricultural Science, Graduate School of Agriculture, Universitas Brawijaya. Jl. Veteran, Malang 65145, East Java, Indonesia. Tel.: +62-341-565845, Fax.: +62-341-5600111, ♥email: kiatgawin22@student.ub.ac.id

[2]Department of Plant Pests and Diseases, Faculty of Agricultural and Forestry Bioindustry, Universitas Brawijaya. Jl. Veteran, Malang 65145, East Java, Indonesia. Tel.: +62-341-565845, ♥♥email: h_gustarno@ub.ac.id

[3]School of Agricultural Sciences, Jiangxi Agricultural University. Nanchang 330045, Jiangxi, China

[4]Innovation and Management Division, Faculty of Natural Resources, Prince of Songkla University. Hat Yai, Songkhla 90110, Thailand

[5]School of Forest, Fisheries and Geomatics Sciences, University of Florida. Gainesville, Florida 32603, United States

Manuscript received: 18 February 2026. Revision accepted: 26 April 2026.

Abstract. *Chatpiyaphat K, Rizali A, Rahardjo BT, Wang J, Ye X, Sittichaya W, Johnson AJ, Hulcr J, Tarno H. 2026. Landmark-based geometric morphometrics as a complementary tool for female identification of* Euplatypus compositus *and* Euplatypus parallelus*. Biodiversitas 27 (4): d270439. https://doi.org/10.13057/biodiv/d270439.* Identification of female Platypodinae ambrosia beetles is often difficult due to strong sexual dimorphism and limited diagnostic characters, particularly in *Euplatypus compositus* and *Euplatypus parallelus*, two closely related species in the southern United States with overlapping habitats and highly similar female morphology. Although the presence or absence of a pronotal mycangial pit is diagnostic, this structure can be obscured by specimen damage. We evaluated landmark-based geometric morphometrics (GM) as a complementary method for distinguishing females of the two species. A total of 46 specimens were analyzed for the pronotum (*E. compositus* n: 17; *E. parallelus* n: 29) and 43 for the elytra (*E. compositus* n: 16; *E. parallelus* n: 27). Multivariate regression revealed significant allometric scaling in pronotum shape (R^2: 18.9%, p: 0.001), whereas elytral shape showed no detectable allometric effect (R^2: 0.7%, p: 0.867). Cross-validated discriminant analysis (LOOCV in XYOM) indicated stronger species discrimination for the pronotum (84.8% accuracy; TAU: 67%) than for the elytra (76.7% accuracy; TAU: 50%), and repeated stratified k-fold cross-validation in R confirmed more robust and consistent discrimination for the pronotum but weaker and more variable performance for the elytra. Geometric morphometrics can detect subtle interspecific differences not apparent through visual inspection and may serve as a complementary identification approach when specimens are well preserved. However, this study demonstrates discriminatory potential under controlled conditions only. Because species identity is confounded with geographic origin and collection history, the observed shape differences, while consistent with species-level variation, cannot be attributed to species identity alone with full confidence. Validation using broader, more balanced sampling remains necessary.

Keywords: Female identification, geometric morphometrics, Platypodinae, pronotum, species discrimination

INTRODUCTION

Platypodinae are ambrosia beetles characterized by an elongated body, short abdomen, and well-developed armature on the elytral declivity (Atkinson 2004). They depend on symbiotic ambrosia fungi for larval development, usually cultivating one or two ascomycete species within galleries (Jordal 2014). These fungi are transported between host plants in specialized mycangia located in the pronotum or coxal cavities. Platypodinae are host generalists that breed in diverse tree families. Although most species cause limited economic damage, their polyphagous behavior can raise management concerns in plantations, especially monocultures vulnerable to infestation. Even one weakened tree may attract beetles, and a few aggressive or invasive species, most notably *Euplatypus parallelus*, can colonize healthy trees and facilitate spread (Gümüş and Ergün 2015). Thus, the disproportionate impact of a few species has contributed to a broader perception of economic importance within the group (Kirkendall and Atkinson 2024).

Euplatypus parallelus, an invasive and economically significant species in many tropical and subtropical regions, including the southern United States, overlaps with the morphologically similar *Euplatypus compositus*. Although *E. compositus* can also cause damage, it is generally less invasive and of lower management concern than *E. parallelus* (Rodrigues et al. 2023), increasing misidentification risk during monitoring. Accurate identification is essential for surveillance and assessment.

Sexual dimorphism is pronounced in many Platypodinae. Adult males often possess distinctive elytral armature, whereas females of some species have blunted or reduced projections (Atkinson 2004). Consequently, taxonomic keys often emphasize male characters, making females difficult to distinguish. This limitation is evident in females of *E. compositus* and *E. parallelus*. American Platypodinae females are particularly difficult to identify because diagnostic

characters are limited (Kirkendall and Atkinson 2024). Although males of these species can be separated by elytral morphology, females are mainly distinguished by the presence (*E. compositus*) or absence (*E. parallelus*) of a pronotal mycangial pit. This structure is visible under a stereomicroscope, but damage or poor preservation can obscure it.

The strong morphological similarity among female Platypodinae has led most taxonomic studies to emphasize males, leaving female morphology under-characterized despite the diagnostic relevance of mycangia (Jordal 2014). This represents a persistent gap in female-based identification. Geometric morphometrics (GM) has proven effective for discriminating cryptic species in fireflies (Sumruayphol and Chaiphongpachara 2019), mosquitoes (Laojun et al. 2025a; Laojun et al. 2025b), and darkling beetles (Tenebrionidae) (Szara et al. 2025), and for examining sexual dimorphism in ambrosia beetles such as *Xyleborus affinis* (Ospina-Garcés et al. 2021). GM quantifies shape using landmark- and outline-based approaches (Laojun et al. 2024a; Laojun et al. 2024b). Landmark-based methods may suit Platypodinae because the pronotum and elytra possess homologous points for repeatable placement.

Although *E. compositus* and *E. parallelus* are separable by subtle pronotal characters (Atkinson 2004), female external morphology is otherwise similar, complicating identification. Molecular identification can resolve ambiguity but is often costly and impractical for routine surveys. GM offers a rapid and cost-effective complementary approach (Rohlf 2002). Because Platypodinae are polyphagous and multiple species may infest the same host tree (Kirkendall and Atkinson 2024), reliable female identification methods are valuable.

In this study, we apply landmark-based geometric morphometrics to pronotal and elytral structures of taxonomic importance (Jordal 2014) to test the hypothesis that subtle but consistent shape differences can discriminate females of *E. compositus* and *E. parallelus*. We further evaluate whether pronotal landmarks provide greater discriminatory power than elytral landmarks. This analysis is intended as a proof-of-concept that first evaluates whether a species-level shape signal can be detected under optimal conditions using well-preserved specimens with clearly identifiable diagnostic characters, prior to future validation on damaged or diagnostically ambiguous material. The objective is to assess whether landmark-based geometric morphometrics can provide a complementary method for distinguishing these closely related species in a geographically diverse sample of specimens under controlled conditions.

The dataset includes specimens drawn from multiple geographic regions to capture population-level morphological variation. However, species identity, geographic origin, and collection history are not fully disentangled in the present dataset. Geographic effects were not explicitly modeled, and the sampling should therefore be interpreted as representing regional diversity rather than a formal test of geographic variation.

MATERIALS AND METHODS

Specimen sources, identification, and imaging

Adult female *E. compositus* and *E. parallelus* specimens (Figure 1) were obtained from the University of Florida Forest Entomology Collection (UFFE), School of Forest, Fisheries, and Geomatics Sciences, and the Florida State Collection of Arthropods (FDACS-DPI), Gainesville, Florida, USA. All specimens were previously identified and curated by FDACS-DPI personnel using standard taxonomic criteria (Table 1 and Table 2). The reliability of species identification in the analyzed material is supported by both expert curation and the clear visibility of the diagnostic pronotal mycangial pit (Rodrigues et al. 2023).

A total of 46 (*E. compositus* n: 17; *E. parallelus* n: 29) pinned specimens were used for pronotum analysis, and 43 (*E. compositus* n: 16; *E. parallelus* n: 27) for elytral analysis. Only well-preserved specimens were included, with the pronotum and elytra fully visible and the elytra in a closed, natural resting position. Specimens were photographed in May 2025 at the School of Forest, Fisheries, and Geomatics Sciences, University of Florida. To minimize imaging-related variation, all specimens were positioned in a standardized dorsal orientation with the longitudinal body axis aligned horizontally in the field of view.

Figure 1. Dorsal view of adult female specimens of (A) *Euplatypus compositus* and (B) *Euplatypus parallelus*. Representative digital micrographs used for morphometric measurements and species comparison. Scale bars: 1.0 mm

Table 1. Catalog numbers of specimens used in geometric morphometric analyses

Species	Collection	Catalog number
Euplatypus compositus	FDACS	FSCA00013841
Euplatypus compositus	FDACS	FSCA00013842
Euplatypus compositus	FDACS	FSCA00013854
Euplatypus compositus	FDACS	FSCA00013855
Euplatypus compositus	FDACS	FSCA00013867
Euplatypus compositus	FDACS	FSCA00013868
Euplatypus compositus	FDACS	FSCA00013881
Euplatypus compositus	FDACS	FSCA00013894
Euplatypus compositus	FDACS	FSCA00013907
Euplatypus compositus	FDACS	FSCA00013920
Euplatypus compositus	FDACS	FSCA00013933
Euplatypus compositus	FDACS	FSCA00013942
Euplatypus compositus	FDACS	FSCA00013946
Euplatypus compositus	FDACS	FSCA00013959
Euplatypus compositus	FDACS	FSCA00013960
Euplatypus compositus	FDACS	FSCA00013972
Euplatypus compositus	FDACS	FSCA00013973
Euplatypus parallelus	FDACS	FSCA00013840
Euplatypus parallelus	FDACS	FSCA00013853
Euplatypus parallelus	FDACS	FSCA00013866
Euplatypus parallelus	FDACS	FSCA00013879
Euplatypus parallelus	FDACS	FSCA00013880
Euplatypus parallelus	FDACS	FSCA00013892
Euplatypus parallelus	FDACS	FSCA00013893
Euplatypus parallelus	FDACS	FSCA00013905
Euplatypus parallelus	FDACS	FSCA00013906
Euplatypus parallelus	FDACS	FSCA00013918
Euplatypus parallelus	FDACS	FSCA00013919
Euplatypus parallelus	FDACS	FSCA00013932
Euplatypus parallelus	FDACS	FSCA00013945
Euplatypus parallelus	FDACS	FSCA00013958
Euplatypus parallelus	FDACS	FSCA00013971
Euplatypus parallelus	UFFE	UFFE44697
Euplatypus parallelus	UFFE	UFFE44698
Euplatypus parallelus	UFFE	UFFE44700
Euplatypus parallelus	UFFE	UFFE44701
Euplatypus parallelus	UFFE	UFFE44702
Euplatypus parallelus	UFFE	UFFE44719
Euplatypus parallelus	UFFE	UFFE44720
Euplatypus parallelus	UFFE	UFFE44721
Euplatypus parallelus	UFFE	UFFE44722
Euplatypus parallelus	UFFE	UFFE44723
Euplatypus parallelus	UFFE	UFFE44725
Euplatypus parallelus	UFFE	UFFE44730
Euplatypus parallelus	UFFE	UFFE44732
Euplatypus parallelus	UFFE	UFFE44733

Note: FSCA: Florida State Collection of Arthropods (FDACS-DPI), Gainesville, Florida, USA. UFFE: University of Florida Forest Entomology Collection, Gainesville, Florida, USA

Imaging was conducted at a fixed magnification and camera distance, with consistent illumination settings to reduce shadowing and glare. The pronotum and elytra were oriented parallel to the imaging plane to minimize distortion due to tilt or rotation. A scale bar was included in all images, which were saved in JPEG format. Prior to landmark digitization, images were visually inspected to ensure consistent orientation and to confirm the absence of noticeable lens distortion. The diagnostic pronotal mycangial pit was clearly visible and unambiguous in all specimens included in this study. Only well-preserved specimens were analyzed, and damaged or diagnostically ambiguous material was excluded. The results, therefore, establish discriminatory potential under controlled conditions and provide a basis for future validation on damaged or diagnostically ambiguous material.

Specimens were examined using an Olympus SZX16 stereomicroscope and photographed at fixed magnification using a Canon EOS R5 digital camera. Images were calibrated using a stage micrometer, and scale bars were included for measurement and landmark digitization. All specimens were imaged under standardized conditions (consistent orientation, magnification, and illumination) to minimize imaging-related variation. Images were captured as single focal planes and adjusted for brightness and contrast without altering diagnostic morphological features. Focus stacking was not performed because landmarks were located on planar or near-planar regions and were consistently visible in a single focal plane. All images were evaluated prior to digitization, and landmark positions were clearly defined and reproducible. Because most landmarks were placed along simple edges with limited three-dimensional complexity, extended depth-of-field imaging was not required. Under these conditions, landmark-based geometric morphometric analyses are considered robust when landmark placement is consistent and repeatable (Adams and Otárola-Castillo 2013).

Body length measurement

Body length was measured from calibrated digital images as the straight-line distance from the anterior margin of the head to the posterior apex of the elytra along the body midline. Each image was calibrated using the visible scale bar prior to measurement. Measurements were performed by a single observer to ensure consistency. Body length was used as a general size reference to support the interpretation of morphometric results.

Study design limitations

The present dataset consisted exclusively of well-preserved museum specimens with clearly visible pronotal mycangial pits, allowing confident species identification prior to morphometric analysis. Consequently, the study does not directly evaluate performance under conditions where diagnostic features are damaged or ambiguous and should be interpreted as an initial assessment of whether consistent interspecific shape differences can be detected in confidently identified material.

Specimens were obtained from multiple geographic regions and collection periods, and representation of the two species was not balanced across locations or time windows (Table 2). Importantly, species identity is confounded with geographic origin and collection history in the present dataset, as *E. compositus* specimens originate exclusively from the United States, whereas *E. parallelus* specimens derive from multiple Neotropical localities. Consequently, the study design does not allow separation of species effects from geographic or collection-history effects. Observed shape differences may therefore reflect a combination of species-level and population-level variation

rather than species identity alone. This limitation is central to the interpretation of the results and should be considered when evaluating discriminatory performance. Future studies incorporating geographically paired sampling or explicitly modeling geographic effects would be required to disentangle these factors.

The relatively limited sample size reflects constraints in specimen availability and standardization requirements. Only specimens with consistent orientation, intact diagnostic structures, and imaging suitable for landmark digitization were included. Although additional material exists in collections, many specimens could not be used due to damage, incomplete preservation, or lack of standardized imaging. Because geometric morphometric analyses require consistent scaling and orientation across specimens, these requirements further restricted the usable dataset. Future studies incorporating broader sampling through coordinated collection efforts and standardized imaging protocols would allow expansion of the dataset.

Digitizing error and repeatability assessment

To evaluate the precision and repeatability of landmark placement, intra-observer digitizing error was assessed separately for the pronotum (n: 46) and elytra (n: 43). Each structure was digitized independently three times by the same observer under consistent magnification and viewing conditions. Landmark coordinates were digitized in XYOM (Dujardin and Dujardin 2019) and exported as two-dimensional X-Y coordinate files, which were imported into R (version 4.5.1) and combined across the three repetitions for each specimen.

Landmark configurations were aligned using Generalized Procrustes Analysis (GPA) to remove the effects of translation, rotation, and scale. Shape variation was partitioned into components attributable to differences among specimens (biological variation) and residual variation (digitizing error) using Procrustes analysis of variance (Procrustes ANOVA) with residual randomization (999 permutations), implemented in the R package geomorph (version 4.0.10). In this model, specimen identity was treated as a factor and the residual term represented within-specimen variation arising from replicate digitization.

The relative contributions of specimen variation and digitizing error were quantified from the sums of squares of the Procrustes ANOVA. Digitizing repeatability (R) was calculated from the ANOVA mean squares and reported as the repeatability of the mean landmark configuration across three replicate digitizations. All analyses were conducted in R using the packages geomorph and RRPP (version 2.1.2).

Landmark-based geometric morphometric analysis

A landmark-based geometric morphometric approach was used to quantify size and shape variation of the pronotum and elytra of *E. compositus* and *E. parallelus*. Six landmarks were digitized on the pronotum and seven on the elytra (Figure 2 and Table 3). Landmarks were positioned on homologous, repeatable anatomical points (e.g., maxima of curvature and sutural or basal reference points) to minimize digitization subjectivity. Most landmarks correspond to Type II landmarks sensu Bookstein (1991), positioned at maxima of curvature or along clearly defined structural boundaries. However, some elytral landmarks are operationally defined based on relative position along smooth margins or surfaces, where discrete anatomical reference points are limited.

These landmarks were selected because they capture key aspects of pronotal and elytral geometry commonly used in Platypodinae taxonomy, including anterior margin curvature, lateral pronotal expansion, and the posterior pronotal boundary relative to the elytral base. Such features are associated with species-level morphological differences in *Euplatypus* and are consistently visible across specimens, making them suitable for repeatable landmark placement. Although the number of available homologous points is limited by the relatively smooth external morphology of these structures, the selected configuration captures the major axes of shape variation relevant to interspecific comparison. Some elytral landmarks are defined by relative position along smooth margins rather than sharply delimited anatomical features, which may contribute to increased digitizing error and reduced repeatability compared to pronotal landmarks.

Table 2. Geographic origin, collection period, and sample sizes of examined specimens

Species	Country	Province/City	N (specimens)	Collection period	Sampling method	Collection
Euplatypus compositus	United States	Florida	9	2010-2014	Light trap, black light trap	FDACS
Euplatypus compositus	United States	Oklahoma	8	1977-1988	Not recorded	FDACS
Euplatypus parallelus	Panama	Barro Colorado Island	5	1967	Light trap	FDACS
Euplatypus parallelus	Dominican Republic	Pedernales	2	2000	Black light trap	FDACS
Euplatypus parallelus	Dominican Republic	Monseñor Nouel	3	1998-2000	Black light trap	FDACS
Euplatypus parallelus	French Guiana	Roura	5	2002	Black light trap, mercury vapor light trap	FDACS
Euplatypus parallelus	Costa Rica	Puntarenas Province	5	2015	Malaise trap	UFFE
Euplatypus parallelus	Paraguay	Paraguarí Dept.	9	2019	Black light trap, mercury vapor light trap	UFFE

Note: Geographic and temporal effects cannot be fully disentangled due to differences in collection regions and periods. Specimens are deposited in the Florida State Collection of Arthropods (FDACS-DPI, Gainesville, Florida, USA) and the University of Florida Forest Entomology Collection (UFFE, Gainesville, Florida, USA)

The number of landmarks was constrained by the availability of clearly homologous anatomical points on the pronotum and elytra; semi landmarks were not employed because boundary curves were weakly defined and could not be homologized consistently across specimens. Because the elytra are bilaterally symmetrical and were imaged in standardized dorsal orientation, landmarks were digitized on one side only to avoid redundancy and reduce digitizing error. This approach is commonly used in geometric morphometric analyses when bilateral symmetry is present and asymmetry is not the focus of the study. Images were uploaded to the XY Online Morphometrics platform (XYOM; https://xyom.io/) (Dujardin and Dujardin 2019) and scaled prior to digitization. Landmark coordinates were collected in XYOM and subjected to Generalized Procrustes Analysis (GPA), principal component analysis (PCA), and exploratory discriminant analysis. Resulting principal component scores were exported for subsequent analyses in R. XYOM was accessed in September 2025. Size was quantified as centroid size (CS), defined as the square root of the summed squared distances of all landmarks from the centroid of the landmark configuration. Differences in centroid size among groups were tested using one-way analysis of variance (ANOVA), with statistical significance further assessed using non-parametric permutation tests (1,000 permutations). Although the number of landmarks was limited, repeatability analysis indicated that digitizing error was substantially smaller than biological variation among specimens, supporting the reliability of the landmark configuration.

Shape analysis

Shape variables obtained from Generalized Procrustes Analysis (GPA) were subjected to principal component analysis (PCA) in the XYOM platform to summarize major patterns of shape variation and reduce dimensionality. For exploratory analyses and visualization, principal components accounting for the full shape variance in the dataset were retained (eight PCs for the pronotum and ten PCs for the elytra), as implemented by XYOM.

Discriminant analysis (DA) based on these PC scores was used as an exploratory assessment of canonical separation between species. The number of PCs included in the discriminant analysis was constrained by the software based on the smallest group size to maintain an appropriate variable-to-sample ratio. Classification performance was subsequently evaluated using cross-validation procedures described below.

Overall shape differences between species were assessed using permutation-based Procrustes ANOVA (1,000 permutations), which operates directly on Procrustes-aligned coordinates and therefore reflects differences in shape as quantified by Procrustes distances.

To quantify multivariate separation among groups, Mahalanobis distances were calculated in canonical discriminant space. Unlike Procrustes distances, which measure absolute shape differences, Mahalanobis distances account for within-group covariance and are therefore appropriate for assessing group separation and classification. Pairwise Mahalanobis distances were assessed using permutation tests (pronotum: 1,087 permutations; elytra: 1,163 permutations) with Bonferroni correction applied for multiple comparisons (α: 0.05).

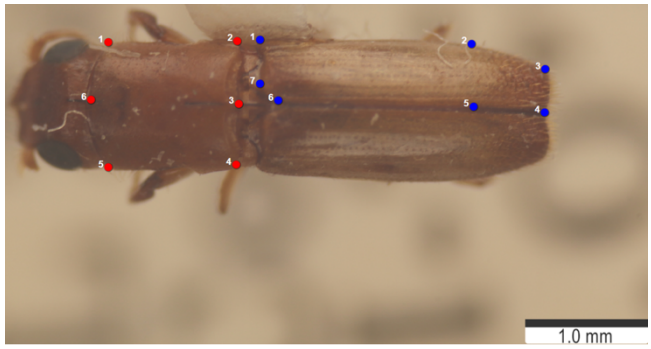

Figure 2. Landmark configuration used for geometric morphometric analysis of the pronotum (red points; 6 landmarks) and elytra (blue points; 7 landmarks) in *Euplatypus*. The illustrated configuration is representative and was applied identically to both *Euplatypus compositus* and *Euplatypus parallelus*. Numbers indicate homologous landmark positions. Scale bar: 1.0 mm.

Table 3. Anatomical definitions of pronotal (6) and elytral (7) landmarks in *Euplatypus parallelus* (adult female, dorsal view)

Land-mark No.	Structure	Anatomical definition
Pronotum landmarks		
1	Pronotum	Left anterolateral margin of the pronotun at the point of maximum curvature near the anterior pronotal edge.
2	Pronotum	Posterodorsal median point of the pronotum at the pronotum-elytra boundary.
3	Pronotum	Right lateral margin of the pronotum at approximately midlength.
4	Pronotum	Right posterolateral margin of the pronotum at the point of maximum curvature.
5	Pronotum	Left posterolateral margin of the pronotum at the point of maximum curvature.
6	Pronotum	Left lateral margin of the pronotum at approximately midlength.
Elytra landmarks		
1	Elytra	Basal sutural point at the anterior elytral margin adjacent to the scutellum.
2	Elytra	Right lateral margin of the elytron at the anterior third of elytral length.
3	Elytra	Right lateral margin of the elytron near the apical third.
4	Elytra	Apicolateral angle of the right elytron.
5	Elytra	Central disc of the right elytron along the longitudinal axis.
6	Elytra	Left discal surface of the elytron at approximately the basal third.
7	Elytra	Basal sutural region of the left elytron adjacent to the elytral base.

Cross-validation and permutation testing

To assess classification performance beyond exploratory discriminant analysis, we conducted repeated stratified k-fold cross-validation (k: 5, 100 repeats) using linear discriminant analysis implemented in R. Principal component scores derived from the PCA performed in XYOM on the full dataset were exported and used as predictor variables for the classification models in R. Stratification preserved the relative proportions of *E. compositus* and *E. parallelus* within each fold. The first five principal components (derived from the full-dataset PCA in XYOM) were retained a priori for each structure, explaining approximately 90-95% of total shape variance while balancing information retention and model stability given the limited sample sizes. Within each resampling iteration, predictor variables were standardized using the mean and standard deviation estimated from the training subset, and the same scaling parameters were applied to the corresponding test subset. Analyses were performed separately for the pronotum and elytral datasets. Because GPA and PCA were performed prior to cross-validation and were not recomputed within each training fold, the resulting accuracy estimates may be optimistic due to potential information leakage between training and test data. This repeated cross-validation framework was treated as an estimate of classification performance under the current analytical design, rather than as fully independent predictive validation, given the limited sample sizes.

Classification accuracy

Leave-one-out cross-validation (LOOCV) was also performed as a secondary, supplementary assessment of classification stability and is not treated as the primary estimate of predictive performance. In this procedure, each specimen was sequentially excluded from the dataset and treated as an unknown sample. Mahalanobis distances between the excluded specimen and group centroids were calculated based on the remaining specimens, and the specimen was assigned to the group with the smallest distance. Group centroids were recalculated at each iteration following the removal of each specimen to avoid circularity and overestimation of classification success. Overall classification accuracy was computed as the proportion of correctly classified specimens. Additionally, the adjusted total accuracy (TAU) was calculated to account for chance-corrected classification, particularly under unequal group sizes. To further address class imbalance, class-wise correct assignment rates (sensitivity) and balanced accuracy (mean class-wise sensitivity) were also examined. Given the limited and unbalanced sample sizes, classification results are interpreted cautiously as estimates of discriminative performance.

Allometry analysis

Allometric relationships were quantified using multivariate regression of Procrustes-aligned coordinates on log-transformed centroid size, following Drake and Klingenberg (2008). Analyses were performed in R using the geomorph package (Adams and Otárola-Castillo 2013).

For each structure (pronotum and elytra), landmark configurations were first aligned using Generalized Procrustes Analysis (GPA), which removes variation due to position, orientation, and scale. Centroid size was extracted during GPA as the square root of the sum of squared distances from each landmark to the configuration centroid. We then fitted a multivariate linear model:

Shape = log(Centroid size)

Where, Shape represents the vector of Procrustes-aligned coordinates. The model was fitted using the function *procD.lm()* with 1,000 permutation iterations to assess statistical significance. The coefficient of determination (R^2) was used to quantify the proportion of shape variation explained by size across all dimensions simultaneously.

Initial allometry assessments were also performed in XYOM using PC-by-PC regression. Although useful for exploratory analysis, this approach has limitations because allometric signal may be distributed across multiple principal components, and PC axes are sample-specific (Drake and Klingenberg 2008). For this reason, both approaches are presented, with multivariate regression considered the primary method for allometry estimation.

RESULTS AND DISCUSSION

Digitizing repeatability assessment

Procrustes ANOVA showed that variation among specimens exceeded digitizing error for both structures (Table 4). In the pronotum dataset, specimen variation accounted for 76.49% of total shape variation, whereas digitizing error contributed 23.51% (F: 6.651, p: 0.001). Similarly, in the elytra dataset, specimen variation explained 67.59% of shape variation, and digitizing error accounted for 32.41% (F: 4.27, p: 0.001). Repeatability estimates were R: 0.850 for the pronotum and R: 0.766 for the elytra, indicating that variation among specimens exceeded variation attributable to replicate digitization. However, the proportion of variation attributable to digitizing error, particularly for the elytra (32.41%), indicates that landmark placement represents a substantial and non-negligible source of variation that should be considered when interpreting shape differences. Landmark placement followed predefined anatomical criteria and was performed by a single trained observer under consistent magnification and viewing conditions to minimize placement variability. Future work could further examine landmark-specific sources of digitizing error and refine landmark definitions where necessary.

Pronotum and elytra size analysis

The average centroid size (CS) of the pronotum and elytra is presented in Table 5, and the distribution of centroid size is shown in Figure 3. No significant differences in centroid size were detected between species for either the pronotum (one-way ANOVA: $F_{1,44}$: 0.499, p: 0.776; permutation ANOVA: p: 0.496) or the elytra (one-way ANOVA: $F_{1,41}$: 0.061, p: 0.969; permutation ANOVA: p: 0.827), indicating that centroid size does not provide discriminatory information between the two species.

Pronotum and elytra shape analysis

The mean shapes of the pronotum and elytra show statistically supported interspecific differences (Figure 4). Visualization of mean landmark configurations indicates that shape differences in the pronotum are primarily associated with subtle lateral expansion and posterior margin displacement, particularly around landmarks 3-5. In contrast, the elytra exhibit more localized and less pronounced landmark shifts, mainly around the posterior-lateral region (landmarks 5-6). These deformation patterns are consistent with the stronger geometric and discriminant separation observed for the pronotum.

Table 4. Procrustes ANOVA results assessing intra-observer digitizing repeatability for pronotal and elytral landmark configurations

Structure	SS (specimen)	SS (error)	% (specimen)	% (error)	F	p	R
Pronotum	0.216874	0.066664	76.49	23.51	6.651	0.001	0.850
Elytra	0.161600	0.077494	67.59	32.41	4.270	0.001	0.766

Table 5. Descriptive statistics of centroid size for adult female *Euplatypus compositus* and *Euplatypus parallelus*

Species	Character	N	Mean (mm)	Range (Min-Max)	Variance (mm²)	SD (mm)
Euplatypus compositus	Pronotum	17	1.698	1.511-1.810	0.004	0.064
Euplatypus parallelus	Pronotum	29	1.713	1.564-1.865	0.005	0.072
Euplatypus compositus	Elytra	16	2.764	2.582-2.947	0.014	0.120
Euplatypus parallelus	Elytra	27	2.755	2.483-2.991	0.014	0.119

Note: N: sample size, Min: minimum, Max: maximum, SD: standard deviation

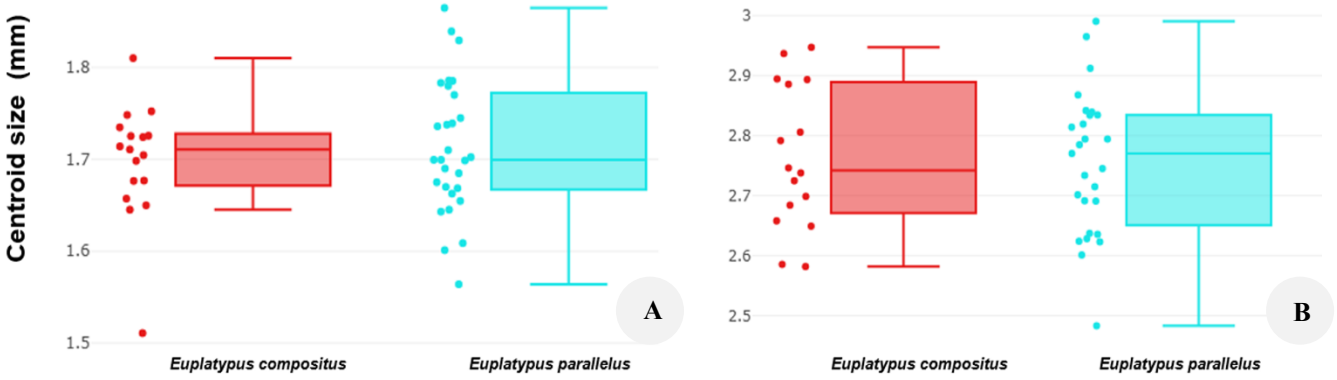

Figure 3. Boxplots of centroid size (mm) for the pronotum (A) and elytra (B) in *Euplatypus compositus* and *E. parallelus*. Each point represents one specimen. Boxes indicate the interquartile range (25th-75th percentiles), the horizontal line denotes the median, and whiskers represent the data range

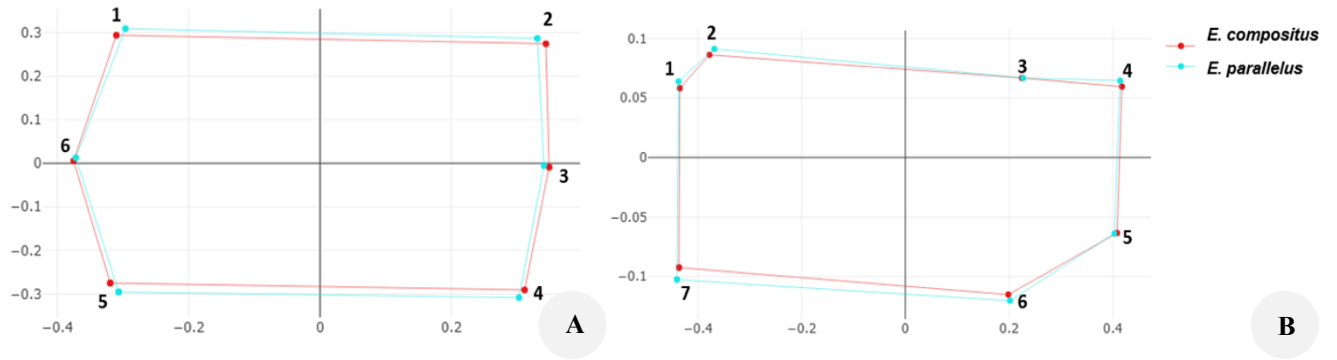

Figure 4. Superposition of mean landmark configurations of *Euplatypus compositus* (red) and *E. parallelus* (light blue) for the pronotum (A: 6 landmarks) and elytra (B: 7 landmarks). Numbers indicate homologous landmarks. Overlaid configurations illustrate average shape differences between species and do not reflect size variation

The Mahalanobis distance was 3.202 for the pronotum (p: 0.001) and 2.585 for the elytra (p: 0.001) (Table 6). Although these results indicate statistically significant differences in mean shape between species, such differences do not necessarily translate into reliable individual-level identification and should be interpreted in conjunction with classification-based performance metrics. The Procrustes distance between mean shapes was 0.001843 for the pronotum and 0.000379 for the elytra, indicating greater geometric differentiation in the pronotum. Canonical discriminant scores indicated clearer separation between species for the pronotum and greater overlap for the elytra (Figure 5), indicating stronger shape differentiation in the pronotum.

Validation of classification performance

Repeated stratified 5-fold cross-validation (100 repeats) confirmed robust discrimination based on pronotum shape (accuracy: 85.6%, SD: 10.5%; balanced accuracy: 83.7%, SD: 12.5%). Permutation testing of cross-validated performance indicated that this discrimination significantly exceeded chance expectations (p: 0.002 for both metrics). For the elytra, cross-validated accuracy was lower and more variable (accuracy: 64.7%, SD: 14.1%; balanced accuracy: 61.1%, SD: 15.0%), and permutation testing did not reach conventional α: 0.05 significance (accuracy p: 0.066; balanced accuracy p: 0.070). These results are consistent with the weaker geometric separation observed for the elytra and indicate that elytral shape provides more limited discriminatory power than the pronotum. Both repeated k-fold cross-validation and supplementary LOOCV analyses consistently ranked the pronotum as providing stronger discriminatory performance than the elytra, although the repeated k-fold framework provides the more conservative and more variable estimate of classification accuracy, better reflecting uncertainty under limited sample sizes.

Supplementary classification (LOOCV)

Supplementary LOOCV-based classification results showed that centroid size alone performed substantially worse than shape-based classification (Table 7). For the pronotum, size-based classification correctly assigned 20 of 46 specimens (43% accuracy; TAU: -21%), whereas shape-based classification correctly assigned 39 of 46 specimens (84.8% accuracy; TAU: 67%). Class-wise correct assignment rates for pronotum shape were 88.2% for *E. compositus* and 82.8% for *E. parallelus*, yielding a balanced accuracy of 85.5%.

A similar pattern was observed for the elytra (Table 8). Size-based classification showed poor discriminatory power (37% accuracy; TAU: -34%), whereas shape-based classification correctly assigned 33 of 43 specimens (76.7% accuracy; TAU: 50%). Class-wise correct assignment rates for elytra shape were 68.8% for *E. compositus* and 81.5% for *E. parallelus*, corresponding to a balanced accuracy of 75.1%. Overall, these results indicate that shape provides substantially stronger discriminatory information than centroid size for both structures. These LOOCV results are presented as supportive evidence and should be interpreted in conjunction with the primary cross-validation results reported above.

Allometry

Allometric effects were assessed using two approaches (Table 9): PC-by-PC regression as implemented in XYOM and multivariate regression of Procrustes coordinates on centroid size in R. Initial PC-by-PC regression suggested minimal allometry in the pronotum (1.3% on PC1, 0.0% on PC2) and moderate allometry in the elytra (4.1% on PC1, 11.6% on PC2). However, this approach is known to be problematic as allometric signal may be distributed across multiple principal components and PC axes are sample-specific (Drake and Klingenberg 2008). We therefore employed multivariate regression of Procrustes-aligned coordinates on log-transformed centroid size, the standard method in geometric morphometrics. This clearly differs from the PC-by-PC estimates (Table 9, Figure 6).

Table 6. Pairwise Mahalanobis distances from geometric morphometric shape analysis between *Euplatypus compositus* and *Euplatypus Parallelus*

Structure	Mahalanobis distance (D2)	p-value
Pronotum	3.202	0.001
Elytra	2.585	0.001

Note: p-values obtained from permutation tests

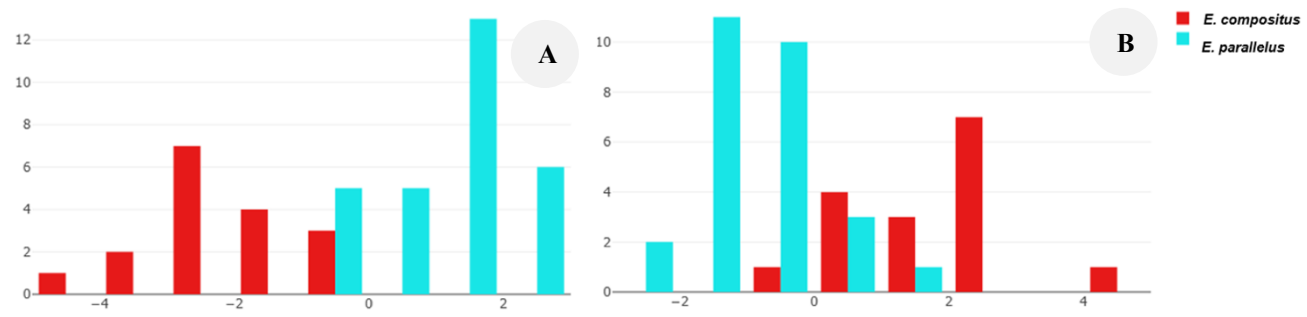

Figure 5. Frequency distributions of individual scores along the first canonical discriminant function for the pronotum (A) and elytra (B) in *Euplatypus compositus* (red) and *E. parallelus* (light blue). Bars represent the number of specimens per score bin. These plots illustrate separation in canonical discriminant space and do not represent classification accuracy

Table 7. Classification performance of the pronotum based on leave-one-out cross-validation (LOOCV)

Actual/Predicted	*Euplatypus compositus*	*Euplatypus parallelus*	Total
Euplatypus compositus	15	2	17
Euplatypus parallelus	5	24	29
Total	20	26	46

Note: Overall accuracy: 39/46: 84.8%; Class-wise correct assignment rate (*E. compositus*): 15/17: 88.2%; Class-wise correct assignment rate (*E. parallelus*): 24/29: 82.8%; Balanced accuracy: 85.5%; TAU (%): 67. TAU (%) = (Observed accuracy − Chance accuracy) / (1 − Chance accuracy) × 100 (McGarigal et al. 2000). Values range from -100 to 100, where values approaching 100 indicate strong discrimination, values near 0 indicate performance close to random classification, and negative values indicate performance worse than random classification. LOOCV results are presented as supportive classification metrics; repeated k-fold cross-validation provides the primary assessment of predictive performance

Table 8. Classification performance of the elytra based on leave-one-out cross-validation (LOOCV)

Actual/Predicted	*Euplatypus compositus*	*Euplatypus parallelus*	Total
Euplatypus compositus	11	5	16
Euplatypus parallelus	5	22	27
Total	16	27	43

Note: Overall accuracy: 33/43: 76.7%; Class-wise correct assignment rate (*E. compositus*): 11/16: 68.8%; Class-wise correct assignment rate (*E. parallelus*): 22/27: 81.5%; Balanced accuracy: 75.1%; TAU (%): 50. LOOCV results are presented as supportive classification metrics; repeated k-fold cross-validation provides the primary assessment of predictive performance

Pronotum shape exhibited strong and significant allometric scaling, with size explaining 18.9% of total shape variation (R^2: 18.9%, p: 0.001, F: 10.25; Figure 6). This regression was performed on pooled data across both species; therefore, the observed size-shape relationship may reflect a combination of interspecific and intraspecific allometric patterns rather than species-specific allometry alone. The positive relationship between regression scores and centroid size indicates systematic shape change with increasing body size. In contrast, elytral shape showed no detectable allometric effect, with size accounting for only 0.7% of shape variation (R^2: 0.7%, p: 0.867, F: 0.30), and regression scores showed no significant relationship with centroid size. The discrepancy between methods demonstrates that pronotum allometry is not adequately captured by the leading principal components (PC1-2), indicating that size-related shape variation is distributed across multiple dimensions of shape space. These results confirm that pronotum morphology is highly size-dependent, whereas elytral shape remains largely invariant across the size range examined.

Discussion

This study evaluated the effectiveness of landmark-based geometric morphometrics (GM) for discriminating between two adults female Platypodinae species, *E. compositus* and *E. parallelus*, using pronotum and elytral shape. Procrustes ANOVA indicated that variation among specimens exceeded digitizing error, supporting the reliability of the landmark data used in the analyses. The non-parametric ANOVA showed significant differences in mean shape between species for both structures (Table 6). Exploratory discriminant analysis indicated separation in canonical space (Figure 5), whereas classification analyses provided estimates of predictive performance (Tables 7-8). These results demonstrate that GM can serve as a complementary quantitative tool to assist species discrimination in Platypodinae, rather than as a standalone identification method.

Although GM also provides size-related information, no significant size difference was detected between species, consistent with previous reports. In morphometric discrimination, shape variables are typically prioritized because size exhibits greater phenotypic plasticity in response to environmental factors such as diet and temperature (Ospina-Garcés et al. 2021). While body size can help narrow identification in Platypodinae taxonomy, it was not informative for separating these two species in the present study. Although pronotum shape exhibited significant allometry, centroid size itself did not differ significantly between species and therefore did not provide direct discriminatory power. This indicates that size-related shape variation occurs within species rather than between species, and thus does not translate into improved species separation. Consequently, size contributes to shape variation but does not independently or indirectly enhance species discrimination in the present dataset.

Pronotum shape exhibited significant allometry, with 18.9% of variation explained by size, indicating that shape changes systematically with body size and that this variation is distributed across multiple dimensions of shape space, making it detectable only through multivariate geometric morphometrics. PC-by-PC regression failed to detect this pattern, reinforcing the importance of multivariate regression for assessing allometry. To our knowledge, quantitative evidence of pronotum allometry in Platypodinae ambrosia beetles remains limited, and the present results provide additional evidence for its occurrence. The developmental or functional basis of this pattern remains unknown and warrants further investigation.

In contrast, elytral shape showed no evidence of allometry. This suggests that selective pressures or developmental constraints may differ between body regions. Elytra may be under stabilizing selection related to flight or protection, favoring shape conservation across sizes, whereas the pronotum may be more developmentally plastic; however, this interpretation should be considered a hypothesis requiring further investigation rather than a direct inference from the present data.

The primary finding of this study is that pronotum shape consistently provides stronger and more reliable species discrimination than elytral shape across all analytical approaches. Supplementary LOOCV-based classification metrics (e.g., TAU) were higher for the pronotum (67%) than for the elytra (50%), where partial overlap was observed

(Figure 5, Tables 7-8). Misclassification remains non-negligible, and these LOOCV-based results should be interpreted as supportive rather than primary evidence of classification performance. In Platypodinae taxonomy, both pronotal and elytral characters are important for species identification (Jordal 2014; Mayers et al. 2022), and GM offers a quantitative framework to augment these established characters. The stronger validation performance of the pronotum relative to the elytra further supports the interpretation that pronotal morphology carries the primary species-discriminatory signal in these taxa. This consistent pattern across exploratory, supplementary, and primary validation analyses establishes pronotum morphology as the dominant source of discriminatory signal in the present dataset.

Applications of GM in insects range from studies of morphological variation (Sarıkaya et al. 2019; Zhang et al. 2019) to diagnostic tools (Smith-Pardo et al. 2025). This study provides evidence that pronotum shape, and to a more limited extent, elytral shape, can assist in the discrimination of female *E. compositus* and *E. parallelus*, although the observed shape separation is consistent with species-level differences but cannot yet be fully disentangled from geographic or collection-history effects. Accordingly, the current results are insufficient to support routine application of this approach to damaged or diagnostically ambiguous specimens without targeted validation under such conditions. Both species are capable of infesting the trunks and branches of recently dead trees, exploit a wide range of host plants, and share overlapping habitats in central Florida (Rodrigues et al. 2023). Given their close relatedness and morphological similarity, careful identification is important in ecological and taxonomic studies. Increasing sample size in future work will improve the robustness and stability of GM-based discrimination, as the moderate TAU values observed here likely reflect sampling limitations.

A limitation of the present study is that specimens of the two species were obtained from different geographic regions and collection periods (Table 2), and these factors were not explicitly modeled. Consequently, some observed shape variation may reflect geographic or population-level differences rather than species identity alone. Future studies incorporating geographically paired sampling or explicitly modeling geographic effects would help disentangle these factors.

Table 9. Estimated influence of size on shape variation (allometry) in the pronotum and elytra of *Euplatypus compositus* and *Euplatypus parallelus* based on landmark-based geometric morphometrics

Structure	n (specimens)	LMs (No landmark)	PC-by-PC regression			Multivariate regression		
			PC1 (%)	PC2 (%)	Total (%)	R2 (%)	p-value	F
Pronotum	46	6	1.3	0.0	1.3	18.9	0.001	10.25
Elytra	43	7	4.1	11.6	15.7	0.7	0.867	0.30

Note: PC-by-PC regression results (PC1 and PC2) are presented for exploratory comparison only and do not represent the total allometric effect. The overall allometric relationship is estimated using multivariate regression across all shape dimensions

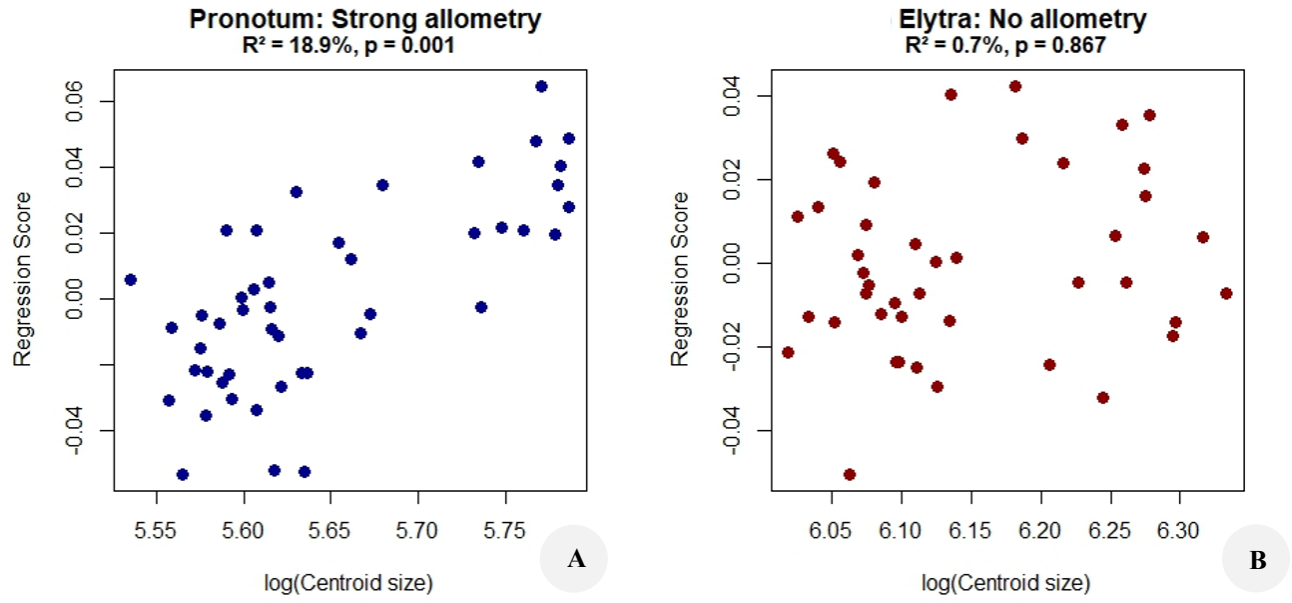

Figure 6. Allometric relationships between size and shape for the pronotum (A) and elytra (B) in *Euplatypus*. Each point represents one specimen plotted by regression score against log-transformed centroid size. The pronotum shows a significant positive relationship (R^2: 18.9%, p: 0.001), whereas the elytra show no significant relationship (R^2: 0.7%, p: 0.867)

The geometric morphometric (GM) approach proposed here is intended to complement, rather than replace, traditional morphological diagnosis. In routine identifications where the mycangial pit is clearly preserved, conventional characters remain sufficient and more straightforward to apply. However, GM may provide additional quantitative support in situations where the mycangial pit is partially obscured, worn, or otherwise difficult to interpret; however, its performance under such conditions has not yet been validated and should be considered provisional. Because the present analysis was conducted under controlled conditions using well-preserved specimens, the performance of GM on damaged material remains to be validated and may depend on whether sufficient homologous landmarks remain visible for consistent placement. Future work is required to evaluate the robustness of this approach under such conditions before it can be considered for routine application in taxonomic or monitoring contexts.

In conclusion, this study demonstrates that landmark-based geometric morphometrics can detect subtle but consistent shape differences between *E. compositus* and *E. parallelus*, supporting its potential use as a complementary approach for species discrimination in Platypodinae. Pronotum shape provided stronger and more reliable separation between species than elytral shape, although the developmental or functional basis of this difference remains unclear. Quantitative morphological analyses may provide a complementary approach when traditional diagnostic characters cannot be evaluated; however, the performance of this approach under such conditions remains to be validated, particularly where sufficient homologous landmarks may not be available for consistent placement. These findings should be interpreted in light of the study design limitations, including limited and geographically unbalanced sampling. Future studies incorporating larger, geographically balanced datasets, damaged material, and independent validation will be necessary to fully assess the robustness and operational utility of geometric morphometrics in ambrosia beetle taxonomy.

ACKNOWLEDGEMENTS

This article has been funded with support of the Kemitraan Negara Berkembang (KNB) Scholarship from Ministry of Higher Education, Sciences, and Technology of Republic of Indonesia on behalf of the Government of the Republic of Indonesia. This publication reflects the view only of the author, and the Ministry of Higher Education, Sciences, and Technology of Republic of Indonesia cannot be held responsible for any use which may be made of the information contained therein. Specimens examined in this study were kindly provided by the Florida State Collection of Arthropods (FSCA) and the University of Florida Forest Entomology Collection (UFFE). We also acknowledge Tanawat Chaiphongpachara (Suan Sunandha Rajabhat University, Thailand) for critical review and constructive feedback on the manuscript, and Nathaniel Levia (School of Forest, Fisheries and Geomatics Sciences, University of Florida, Gainesville, USA) for technical assistance and support with photographic imaging.

REFERENCES

Adams DC, Otárola-Castillo E. 2013. Geomorph: An R package for the collection and analysis of geometric morphometric shape data. Methods Ecol Evol 4: 393-399. https://doi.org/10.1111/2041-210X.12035.

Atkinson TH. 2004. Ambrosia Beetles, *Platypus* spp. (Insecta: Coleoptera: Platypodidae) (EENY-174). University of Florida IFAS Extension, Forida, US. https://ask.ifas.ufl.edu/publication/IN331.

Bookstein FL. 1991. Morphometric Tools for Landmark Data: Geometry and Biology. Cambridge University Press, Cambridge.

Drake AG, Klingenberg CP. 2008. The pace of morphological change: Historical transformation of skull shape in St Bernard dogs. Proc R Soc B Biol Sci 275 (1630): 71-76. https://doi.org/10.1098/rspb.2007.1169.

Dujardin S, Dujardin JP. 2019. Geometric morphometrics in the cloud. Infect Genet Evol 70: 189-196. https://doi.org/10.1016/j.meegid.2019.02.018.

Gümüş EM, Ergün A. 2015. Report of a pest risk analysis for *Platypus parallelus* (Fabricius, 1801) for Turkey. EPPO Bull 45: 112-118. https://doi.org/10.1111/epp.12190.

Jordal BH. 2014. Platypodinae. In: Leschen R, Beutel R (eds). Handbook of Zoology. Arthropoda: Insecta: Coleoptera, Morphology and Systematics (Phytophaga). De Gruyter Press, Berlin/New York.

Kirkendall LR, Atkinson TH. 2024. What we do and don't know about Neotropical pinhole borers (Coleoptera: Curculionidae: Platypodinae). Nor J Entomol Suppl 4: 25-92.

Laojun S, Changbunjong T, Kaewthamasorn M, Charnwichai P, Kaewmee S, Wichit S, Chaiphongpachara T. 2025a. Accurate identification of medically important *Aedes* mosquitoes (Diptera: Culicidae) in Thailand through DNA barcoding, wing geometric morphometrics, and machine learning. Curr Res Parasitol Vector Borne Dis 8: 100334. https://doi.org/10.1016/j.crpvbd.2025.100334.

Laojun S, Changbunjong T, Kamoltham T, Chaiphongpachara T. 2025b. An integrative approach to DNA barcoding, geometric morphometrics, and machine learning for field identification of *Culex* mosquitoes (Diptera: Culicidae), with implications for vector-borne disease surveillance. Acta Trop 271: 107885. https://doi.org/10.1016/j.actatropica.2025.107885.

Laojun S, Changbunjong T, Sumruayphol S, Chaiphongpachara T. 2024a. Outline-based geometric morphometrics: Wing cell differences for mosquito vector classification in the Tanaosri mountain range, Thailand. Acta Trop 250: 107093. https://doi.org/10.1016/j.actatropica.2023.107093.

Laojun S, Changbunjong T, Sumruayphol S, Pimsuka S, Chaiphongpachara T. 2024b. Wing geometric morphometrics and DNA barcoding to distinguish three closely related species of *Armigeres* mosquitoes (Diptera: Culicidae) in Thailand. Vet Parasitol 325: 110092. https://doi.org/10.1016/j.vetpar.2023.110092.

Mayers CG, Harrington TC, Biedermann PH. 2022. Mycangia define the diverse ambrosia beetle-fungus symbioses. In: Schultz TR, Gawne R, McGhee GR (eds). The convergent evolution of agriculture in humans and insects. MIT Press, Cambridge.

McGarigal K, Cushman SA, Stafford SG. 2000. Multivariate Statistics for Wildlife and Ecology Research. Springer, New York.

Ospina-Garcés SM, Ibarra-Juarez LA, Escobar F, Lira-Noriega A. 2021. Evaluating sexual dimorphism in the ambrosia beetle *Xyleborus affinis* (Coleoptera: Curculionidae) using geometric morphometrics. Fla Entomol 104 (2): 61-70. https://doi.org/10.1653/024.104.0201.

Rodrigues A, Johnson AJ, Joseph RA, Li Y, Keyhani NO, Stanley EL, Hulcr J. 2023. Fungal symbiont community and absence of detectable mycangia in invasive *Euplatypus ambrosia* beetles. Symbiosis 90 (3): 305-319. https://doi.org/10.1007/s13199-023-00938-4.

Rohlf FJ. 2002. Geometric morphometrics in systematics. In: Macleod N, Forey P (eds). Morphology, Shape and Phylogenetics. Taylor and Francis, London.

Sarıkaya AD, Okutaner AY, Sarıkaya Ö. 2019. Geometric morphometric analysis of pronotum shape in two isolated populations of *Dorcadion anatolicum* Pic, 1900 (Coleoptera: Cerambycidae) in Turkey. Turk J Entomol 43 (3): 263-270. https://doi.org/10.16970/entoted.525860.

Smith-Pardo AH, Lupoli R, Benítez HA. 2025. Geometric morphometrics as a diagnostic tool for cryptic agricultural pests: Insights from *Nezarini* stink bugs (Hemiptera: Heteroptera: Pentatomidae). J Entomol Sci 61 (2): 1-16. https://doi.org/10.18474/JES25-29.

Sumruayphol S, Chaiphongpachara T. 2019. Geometric morphometrics as a tool for three species identification of the firefly (Coleoptera: Lampyridae) in Thailand. Biodiversitas 20 (8): 2388-2395. https://doi.org/10.13057/biodiv/d200837.

Szara T, Kamiński MJ, Gündemir O. 2025. Exploring desert-adapted beetles with 3D geometric morphometrics. Sci Rep 15: 22824. https://doi.org/10.1038/s41598-025-05967-1.

Zhang M, Ruan Y, Wan X, Tong Y, Yang X, Bai M. 2019. Geometric morphometric analysis of the pronotum and elytron in stag beetles: Insight into its diversity and evolution. ZooKeys 833: 21. https://doi.org/10.3897/zookeys.833.26164.